

# DEVELOPMENT OF TRANSPARENT LSCO AND LSCNO CONDUCTORS FOR OPTICAL SHUTTER SYSTEMS

R. W. Schwartz, M. T. Sebastian, M. Charoenwongsa, and H. D. Dobberstein  
The Gilbert C. Robinson Department of Ceramic and Materials Engineering  
Clemson University  
Clemson, SC

## ABSTRACT

We have prepared lanthanum strontium cobalt oxide ( $\text{La}_{0.50}\text{Sr}_{0.50}\text{CoO}_3$ ; LSCO 50/50) and lanthanum strontium cobalt nickel oxide ( $\text{La}_{0.50}\text{Sr}_{0.50}\text{Co}_{0.50}\text{Ni}_{0.50}\text{O}_3$ ; LSCNO) as candidate transparent electrodes for use in a shutter-based infrared sensor protection device. The shutter device requires that the electrode be transparent (80% transmission) and have moderate sheet resistance (300  $\Omega/\text{sq.}$ ). Because of the effects of film thickness on intrinsic material properties, such as resistivity and extinction coefficient, and simple engineering issues (i.e., the relationship between film thickness, resistance and transmission), films of various thicknesses were prepared to achieve an optimal balance of electrical and optical performance. van der Pauw measurements and FTIR spectroscopy were used to study thin film properties. The best LSCO films prepared demonstrated electrical (438  $\Omega/\text{sq.}$ ) and optical (68% transmission at 8  $\mu\text{m}$ ) properties that did not meet the target property goals for this application. However, the LSCNO films (of optimal thickness) offered performance (323  $\Omega/\text{sq.}$  and 73% transmission) close to the device requirements.

## INTRODUCTION

“Optical” information obtained by sensors such as IR imaging systems is becoming of increasing importance in battlefield management. At the same time, the threat of damage to these optical systems has increased. The protection of sensor systems is therefore becoming more important. While the U.S. and other governments have agreed to prohibit the use of weapons that are designed to cause blinding, the use of tunable lasers by terrorist organizations still poses a significant threat to military personnel and sensor systems [1]. Hence, devices that provide optical limiting and serve to protect sensor systems that operate between 3 – 5 and 8 – 12  $\mu\text{m}$  are of great importance to the U.S. Military.

One sensor protection approach is an electrostatically driven shutter [2,3] placed in the optical path of the sensor, as illustrated in Fig. 1. A device, such as a photodiode, can be used to sense incoming threats and can activate to close the shutter for protection of the sensor. Stringent material requirements are placed on shutter components such as the substrate, electrode, and insulating layer. These layers need to be highly transparent to minimize the reduction in device sensitivity when the shutter is open, but the electrode must possess an adequate conductivity to electrostatically close the shutter. Target goals for the electrode are 80% transmission and a sheet resistance of 300  $\Omega/\text{sq.}$

This paper reports on the electrical and optical properties of lanthanum strontium cobalt oxide (LSCO) and lanthanum strontium cobalt nickel oxide (LSCNO) films prepared for the shutter-based sensor protection device. Although LSCO is known to be absorbing in the visible spectrum, little data is available on its optical properties in the IR region. Other studies indicated the balance between the optical and electrical properties of LSCO could be altered by varying the post-deposition annealing temperature [4,5]. In addition, it has been shown that the plasma edge of oxide conductors such as  $\text{SnO}_2$  can be shifted further into the IR by decreasing the

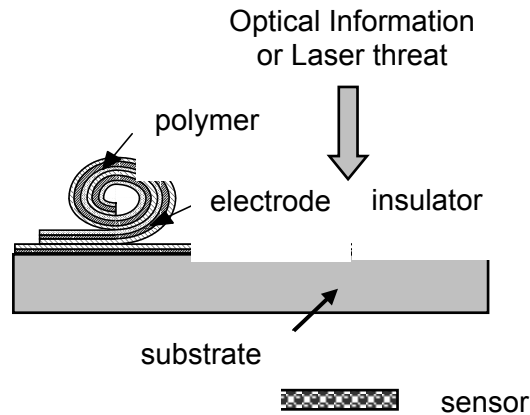


Fig. 1. Schematic of an electrostatic shutter for the protection of optical sensor systems [3].

conductivity of the material [6]. For these reasons, our research has focused on perovskite oxide conductors, such as LSCO. We have studied the effects of a-site/b-site stoichiometry, a-site deficiency, and film thickness on electrical and optical properties. Because  $\text{LaNiO}_3$  [7] has been reported to demonstrate high conductivity, we have also explored the properties of Ni-doped LSCO films, in particular,  $\text{La}_{0.50}\text{Sr}_{0.50}\text{Co}_{0.50}\text{Ni}_{0.50}\text{O}_3$ .

## EXPERIMENTAL

The LSCO thin films were prepared by sol-gel processing and rf-magnetron sputtering while the LSCNO films were prepared solely by sputtering. For the sol-gel solutions, the typical batch size was 30 ml with equal amounts of acetic acid and 2-methoxyethanol and the concentration of the LSCO was between 0.2 and 0.4 M. Cobalt acetate was dissolved in acetic acid by stirring and heating at  $70^\circ\text{C}$  for 30 minutes. Then, strontium acetate was added and the solution was heated and stirred at  $70^\circ\text{C}$  for an additional 30 minutes. The lanthanum precursor solution was prepared by dissolving lanthanum isopropoxide in 2-methoxyethanol and heating at  $70^\circ\text{C}$  for 30 minutes before mixing with the Co/Sr solution. The combined solution was stirred and heated at the same temperature for another 20 minutes and was then cooled prior to use. Films were prepared within two hours of solution preparation on  $\text{LaAlO}_3$  and  $\text{MgO}$  by spin-casting at 3000 rpm for 30 seconds, followed by pyrolysis at  $300^\circ\text{C}$ , and a crystallization anneal at temperatures between 700 and  $1000^\circ\text{C}$  for 60 minutes.

Sputter deposited LSCO and LSCNO films were prepared from stoichiometric oxide targets using a Kurt J. Lesker system equipped with a 3" gun. A deposition pressure of 10 – 40 mtorr with a 50/50  $\text{Ar}/\text{O}_2$  atmosphere was maintained, and a sputtering power of 200 watts with a substrate – target distance of 3 – 5 cm was employed. The system was evacuated to a background pressure in the range of  $10^{-7}$  torr prior to deposition. LSCO and LSCNO films were deposited onto (100)  $\text{MgO}$ , and film thickness was varied through deposition time. The LSCO films were annealed after deposition at temperatures between 800 and  $850^\circ\text{C}$  for times of 30 to 60 minutes. The LSCNO films were not annealing following ambient temperature deposition.

The resistivity of the films was characterized using the van der Pauw method and infrared transmission properties were studied with a Nicolet Magna550 spectrometer by subtracting the substrate transmission characteristics as the background. Thickness of the films was determined either by cross-sectional SEM method or by using the SEM results to calculate the sputtering rate, and then specifying the sputter deposition time. Film composition was not characterized, but prior investigations have indicated it may vary during deposition [4].

## RESULTS AND DISCUSSION

Before studying effects of film thickness on electrical and optical properties, the annealing conditions that yielded the best balance of properties for LSCO were evaluated. Table I summarizes the results of this earlier study [5] in terms of the *maximum* film thickness that will permit 80% transmission and the *minimum* film thickness required to achieve a sheet resistance of 300  $\Omega$ /sq. Despite the fact that the electrical and optical properties change with annealing temperature, with both resistance and transmission decreasing with increasing temperature, the best opportunity to use LSCO in this application is to anneal the films at 800°C. Under these processing conditions, the minimum thickness to meet the electrical property requirement is less than the maximum thickness tolerable for the optical property requirement. While these results are encouraging, they neglect the fact that the intrinsic properties of the films will likely degrade as thickness is decreased. Therefore, after identification of optimal processing conditions, LSCO films with thicknesses from  $\sim$  20 to 200 nm were prepared, and the transmission and resistance were characterized.

The results of the thickness investigation are summarized in Fig. 2, which shows the transmission of the films as a function of their resistance. We report “engineering” (transmission and sheet resistance) results here, as opposed to intrinsic properties (extinction coefficient and resistivity), because both the intrinsic electrical and optical properties may vary as a function of thickness. By plotting the results in this fashion, a more straightforward determination of the ability of a given film to provide the required performance balance for this application is permitted. As expected, with increasing film thickness, the sheet resistance of the films decreases, as does transmission. This figure shows it was not possible to tailor film thickness to meet the required balance of electrical and optical properties. The “optimal” film thickness resulted in a transmission of  $\sim$  65% and a sheet resistance of about 450  $\Omega$ /sq. It may also be seen that there is little difference between the performance of the sputtered and sol-gel films. The reasons for this similarity are not fully understood, especially considering the microstructures of the films are quite different. The sol-gel films possess microstructures characterized by 40 – 90 nm grains (depending on thickness) and some porosity [8], while the sputtered films are dense and featureless. The use of MgO substrates for the sputtered films and LaAlO<sub>3</sub> for the sol-gel films may contribute to the observed results because MgO is less well lattice matched to LSCO. The sol-gel films are also annealed at slightly higher temperature.

Though Fig. 2 shows the performance range that may be achieved by preparing films of different thickness, it does not demonstrate any change in intrinsic properties that may be present. We have therefore studied resistivity as a function of thickness, and the results are presented in Fig. 3. As anticipated, as thickness decreases, the intrinsic resistivity of the film increases; i.e., the electrical properties are degraded for thinner films. We have attempted to model this behavior by assuming that the film consists of two regions: a degraded region at the

---

Table I. Opportunities for engineering the resistance and transparency of sputter-deposited LSCO thin films through control of annealing conditions [5].

Post-Deposition Annealing Temp. (°C)	Maximum Thickness for 80% Trans. (nm)	Minimum Thickness for 300 $\Omega$ /sq. (nm)
As-Deposited	180	5670
500	74	350
600	16	43
800	14	9

---

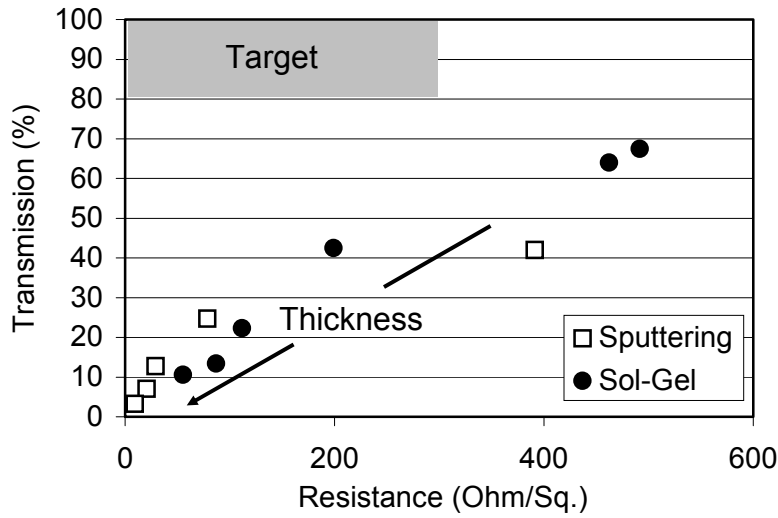


Fig. 2. Percent transmission and sheet resistance of  $\text{La}_{0.50}\text{Sr}_{0.50}\text{CoO}_3$  (LSCO 50/50) films prepared by sputtering and sol-gel processing for films with different thickness. The sputtered films were annealed at  $850^\circ\text{C}$  while the sol-gel films were annealed at  $900^\circ\text{C}$ . Transmission values are at  $3\ \mu\text{m}$  for the sol-gel films and  $8\ \mu\text{m}$  for the sputtered films.

substrate interface and a second region characterized by properties that are more representative of the bulk material. The resistivity of the film was thus modeled as two resistors in parallel using Eqn. 1:

$$\rho_{TOT} = \left( \frac{d_{INT}}{\rho_{INT}} + \frac{d_{BULK}}{\rho_{BULK}} \right)^{-1} * d_{TOT} \quad (1)$$

where  $\rho_{TOT}$  is the overall (measured) resistivity of the film,  $d_{INT}$  and  $\rho_{INT}$  are the thickness and resistivity of the interfacial layer, respectively,  $d_{BULK}$  and  $\rho_{BULK}$  are the thickness and resistivity of the upper, non-degraded layer, respectively, and  $d_{TOT}$  is the total thickness of the film. A range of values for these parameters were evaluated and a reasonable fit to the observed results was

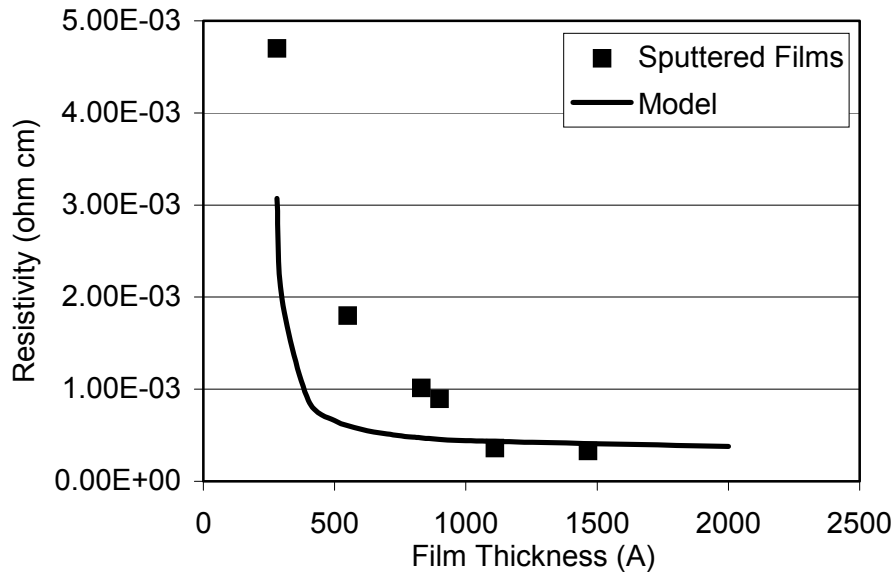


Fig. 3. Resistivity of sputtered and annealed ( $850^\circ\text{C}$ ) LSCO 50/50 thin films. The line represents the predicted resistivity vs. thickness for the two layer model.

obtained for  $d_{INT}$  of  $250\text{\AA}$ ,  $\rho_{INT}$  of  $1\ \Omega\text{cm}$ , and  $\rho_{BULK}$  of  $330\ \mu\Omega\text{cm}$ . Although the model does not perfectly fit the results, it suggests there is an interfacial layer present with relatively poor electrical conductivity, and that when film thickness decreases, the presence of this layer contributes to the observed degradation in properties.

Fig. 4 illustrates the effects of film thickness on the properties of LSCNO films. Because we have not yet determined the thicknesses of these films, the properties are presented as a function of sputtering time. The results for resistance suggest a similar behavior to that observed for the LSCO films; i.e., there appears to be an interfacial layer that contributes to a degradation in electrical properties. Interestingly, the optical properties show a different behavior with a more linear relationship between transmission and sputtering time. We note that these properties are for LSCNO films that were not annealed following the ambient temperature deposition.

The performance of the LSCO and LSCNO films are compared in Fig. 5. The LSCNO films demonstrate greater transmission than LSCO films of equivalent sheet resistance. It is also evident that the LSCNO films come much closer to meeting the target goals for this application. The LSCNO film with the optimal thickness demonstrated a sheet resistance of  $323\ \Omega/\text{sq.}$  and 73% transmission. A slightly thinner film displayed a sheet resistance of  $352\ \Omega/\text{sq.}$  and 81% transmission. LSCNO films thus nearly meet the requirements for the shutter protection device.

The electrical/optical performance of LSCO, LSCNO, and other materials may be compared using a figure of merit (FOM) as described by Jain and Kulshreshtha [9] in Eqn. 2:

$$\text{FOM} = -R_{Sq} \ln T \quad (2)$$

where  $R_{Sq}$  is the sheet resistance in  $\Omega/\text{sq.}$  and  $T$  is the fraction of incident radiation that is transmitted. Here, lower FOM values indicate better performance. The LSCNO materials demonstrate FOM values between 75 and 122 while the LSCO films demonstrate values between 155 and 400. For LSCO, the better FOM values reported were obtained for materials prepared with a-site deficiency  $((\text{La}_{0.50}\text{Sr}_{0.50})_{0.90}\text{CoO}_3)$  [8].

The FOM values may be compared to calculated FOM values for commonly employed materials, such as indium tin oxide. This material demonstrates 80 to 90 % transmission in the visible with a sheet resistance of  $5 - 10\ \Omega/\text{sq.}$  Using Eqn. 2, a FOM for ITO in the visible spectral region is about 1. While caution must be used in the comparison of these materials

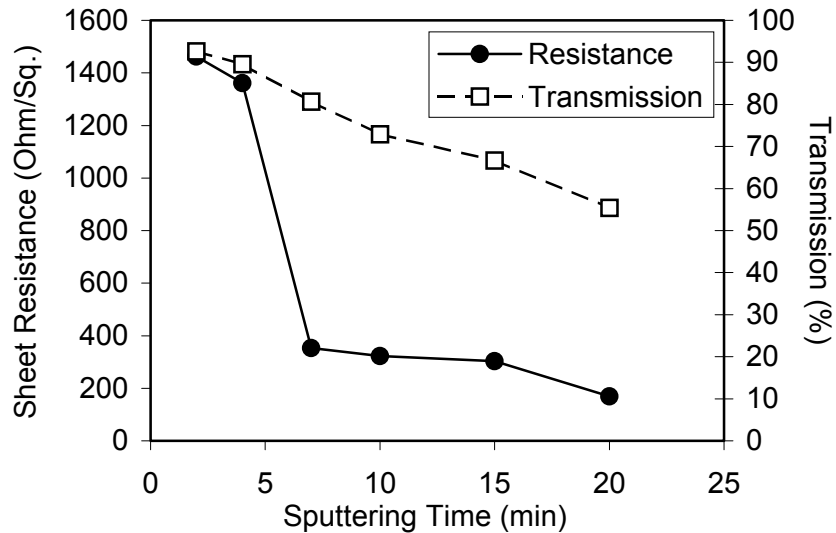


Fig. 4. Percent transmission and sheet resistance of as-deposited LSCNO films prepared with different sputtering times. Transmission values are at  $8\ \mu\text{m}$ .

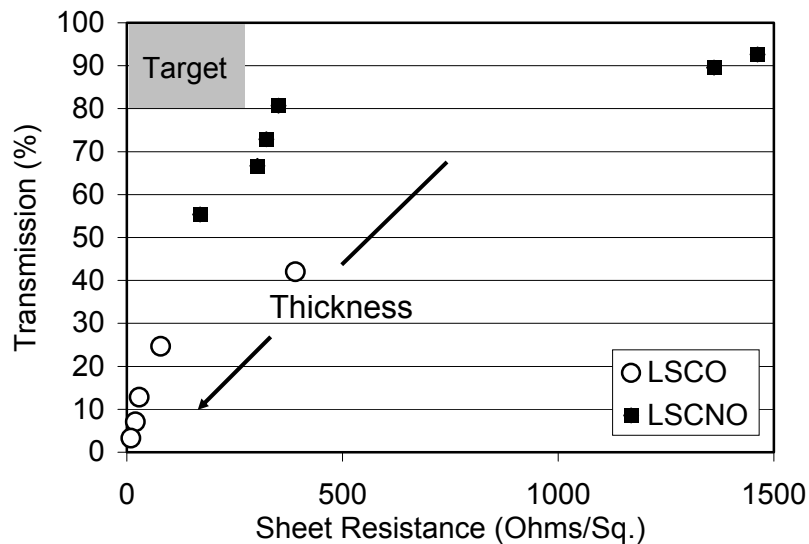


Fig. 5. Percent transmission and sheet resistance of LSCO and LSCNO films with different thicknesses prepared by sputtering. Transmission values are at 8  $\mu\text{m}$ . LSCO films post-deposition annealed at 850°C; LSCNO results reported for as-deposited films.

because of the different spectral regions of interest, the results seem to imply that there are significant opportunities for the development of improved transparent conductors for IR applications. A review of the literature suggests, however, that the LSCNO materials are potentially as attractive as other materials that have been investigated for these wavelengths [10].

## CONCLUSIONS

We have investigated the possible use of LSCO and LSCNO thin films for an IR sensor protection device. The LSCNO films displayed a better balance of electrical and optical properties and did not require a post-deposition annealing step to attain low sheet resistance while maintaining high IR transparency. By controlling film thickness, it was possible to prepare a film with 73% transmission and 323  $\Omega/\text{sq}$ . sheet resistance.

## ACKNOWLEDGMENTS

This work was supported by the U.S. Defense Advanced Research Projects Agency (DARPA) under contract DAAD19-00-1-0002.

## REFERENCES

1. J. S. Shirk, *Optics & Photonics News*, April (2000), p. 19.
2. C. G. Kalt, U.S. Patent 3,989,357 (1975).
3. S. Goodwin-Johansson, et al. *Proc. SPIE*, **3987**, 225 (2000).
4. M. V. Raymond, et al., *Mat. Res. Soc. Symp. Proc.*, **433**, 145 (1996).
5. R. Schwartz, M. Sebastian, and M. Raymond, *Mat. Res. Soc. Symp. Proc.*, **623**, 149 (2000).
6. D. S. Ginley and C. Bright, *Mat. Res. Soc. Bull.*, **25** [8], 15 (2000).
7. M. S. Hedge, et al., *J. Mat. Res.*, **9**, [4], 898 (1994).
8. M. Charoenwongsa, M.S. Thesis, Clemson University (2000).
9. V. K. Jain and A. P. Kulshreshtha, *Solar Ener. Mat.*, **4** [2], 151 (1981).
10. C. F. Windisch, Jr., K.F. Ferris, and G.J. Exarhos, *J. Vac. Sci. Technol.*, **A19** [4], 1 (2001).